Analytical Biochemistry 638 (2022) 114510

Contents lists available at ScienceDirect

Analytical Biochemistry

journal homepage: www.elsevier.com/locate/yabio

Split-luciferase complementary assay of NLRP3 PYD-PYD interaction indicates inflammasome formation during inflammation

Mohsen Isazadeh [a], Mojdeh Amandadi [a], Farnaz Haghdoust [a], Shima Lotfollazadeh [b], Mar Orzáez [c], Saman Hosseinkhani [a,*]

[a] Department of Biochemistry, Faculty of Biological Sciences, Tarbiat Modares University, Tehran, Iran
[b] Department of Nanobiotechnology, Faculty of Biological Sciences, Tarbiat Modares University, Tehran, Iran
[c] Laboratory of Peptide and Protein Chemistry, Centro de Investigación Príncipe Felipe, Valencia, Spain

ARTICLE INFO

Keywords:
Inflammation
Pyroptosis
Inflammasome
NLRP3
PYD domain
Luciferase

ABSTRACT

The NLRP3 inflammasome is a key macromolecular complex of the innate immune system that activates the inflammatory signalling cascade in response to a wide range of stimuli. Structural studies have shown that the intracellular cytosolic receptor NLRP3 oligomerizes upon stimulation and serves as a scaffold to form the ASC filaments necessary for procaspase-1 activation. Despite the abundant structural evidences on NLRP3 inflammasome, the interactions of the NLRP3 Pyrin domain and its functional relevance are poorly understood. In this study, the split luciferase complementation assay is used as an alternative approach to investigate $NLRP3^{PYD}$-$NLRP3^{PYD}$ interactions during inflammasome formation. Since the homotypic NLRP3 interaction is mainly based on electrostatic interactions, a phosphomimetic residue (S5) at the interface of the $NLRP3^{PYDs}$ interactions has been mutated to show a disruptive effect on luciferase activity. According to the results presented, the designed biosensor was able to monitor the $NLRP3^{PYD}$-$NLRP3^{PYD}$ interaction *in vitro*. The current reporter assay not only provides a specific $NLRP3^{PYD}$-$NLRP3^{PYD}$ assay to study the PYD-PYD interaction *in vitro*, but also provides a suitable system for screening chemicals and drugs to identify activators and inhibitors of NLRP3.

1. Introduction

Activation of inflammasome as a core component of the innate immune system in response to a wide range of damage and pathogen associated molecules implicate as a mechanism of body defence. However, the extreme activity of inflammasome primes to autoinflammatory disorders and autoimmune diseases such as, type 1 diabetes, multiple sclerosis (MS), and rheumatoid arthritis (RA) [1,2].

Most typical inflammasomes consist of three main parts: one sensor compartment such as NLRP3, an adaptor protein like ASC, and an effector caspase such as caspase-1 [3,4]. The NLRP3 inflammasome complex promotes proteolytic cleavage of procaspase-1 to caspase-1. Then, activated caspase-1 induces an inflammatory response through interleukin1β (IL-1β) and IL-18 secretion and drives the cell to pyroptotic cell death by cleavage of Gasdermin-D [5].

NLRP3 has a Pyrin Domain (PYD) with a high affinity for homotypic interactions. The crystal structure of the NLRP3 Pyrin Domain ($NLRP3^{PYD}$), procaspase-1 zymogen domain and ASC have been identified in previous studies [6–8]. Also, the interactions between the NLRP3 inflammasome components and the amino acids involved in these interactions are known [9–12]. In the ASC-dependent inflammasomes, upstream sensor proteins, such as NLRP3, recruit ASC through the interaction between their PYD domains. Then, ASC interacts and activates procaspase-1 through CARD-CARD interactions. Therefore, the dual nature of ASC forms the central structure of the inflammasomes [13]. Previous reports have shown that the self-association of NLRP3 and NLRP3 interaction with ASC are mediated through some partially identical binding regions [10].

Until now, three-dimensional structures of more than 10 different PYD domains have been reported in the Protein Data Bank (PDB) [6, 14–23], but our understanding on $NLRP3^{PYD}$-$NLRP3^{PYD}$ homotypic interactions is not so clear. Considering the significant importance of inflammasome complexes and pyroptosis as a vital process, it would be valuable to study this process and developing methods which provide

Abbreviations: ASC, Apoptosis-associate Speck-like protein containing a Caspase recruitment domain; NLRP3, Nucleotide-binding domain and Leucine-rich repeat containing (NLR) Protein 3; PYD, Pyrin Domain; CARD, Caspase Recruitment Domain; Luc, Luciferase; IL, interleukin.

* Corresponding author.
E-mail address: saman_h@modares.ac.ir (S. Hosseinkhani).

https://doi.org/10.1016/j.ab.2021.114510
Received 28 July 2021; Received in revised form 29 October 2021; Accepted 30 November 2021
Available online 1 December 2021

more information about complex assembly and interactions between the inflammasome compounds.

Split-luciferase complementary assay has been used to investigate protein-protein interactions during complex formation. This approach is based on reconstruction of dissected luciferase fragments. Each fragment of the luciferase is fused to one of interacting proteins. Proximity of luciferase fragments upon the interaction of target proteins converts to bioluminescence, which can be quantitatively measured by photon counting. This procedure represents the important benefit of providing a signal with low background noise [24,25]. Split luciferase complementary assay has been used to show the Apaf1-Apaf1 interaction during apoptosome formation both *in vitro* and *in vivo* conditions [26–29].

In the current study, a biosensor is designed based on split luciferase complementation to study the specific intramolecular NLRP3^{PYD}-NLRP3^{PYD} interaction that involved in NLRP3 inflammasome complex formation. The split luciferase fragments of 1–416 amino acids (NLuc) and 395–550 amino acids (CLuc) have been developed and used to make split reporters according to this technology [26,30]. To corroborate the reporting abilities of split luciferase complementary system in response to NLRP3^{PYD}-NLRP3^{PYD} interaction, NLRP3^{PYD} mutants [NLuc-NLRP3-^{PYD} S5D and CLuc-NLRP3^{PYD} S5D] were constructed as a negative control. Also, since the NLRP3 interacts with ASC through some partially identical binding regions, ASC was used as a competitive inhibitor of interactions between NLuc-NLRP3^{PYD} and CLuc-NLRP3^{PYD}. This is the first report on application of split-luciferase complementation assay to investigate the interaction between components of the inflammasome complex.

2. Materials and methods

2.1. Design and cloning of constructs

The N-terminal (NLuc: 1–1248 bp) and C-terminal (CLuc: 1183–1650 bp) fragments of luciferase were PCR-amplified from pGL3 vector encoding *P. pyralis* luciferase (Promega) with appropriate primers. Based on previous reports [31,32], a flexible Gly and Ser linker joined to the reverse primers of NLuc and CLuc. Amplification was also added restriction enzyme sites of *Nde*I/*Sal*I and *Nde*I/*Nde*I to the NLuc and CLuc fragments, respectively. The purified NLuc and CLuc fragments were digested by *Nde*I/*Sal*I and *Nde*I/*Nde*I, and then cloned into the *Nde*I/*Sal*I and *Nde*I/*Nde*I digested/dephosphorylated pET28a (+) vectors. In the next step, the purified NLRP3^{PYD} gene was modified by PCR to introduce restriction enzyme sites of *Sal*I (NLuc-NLRP3^{PYD}) and *Eco*RI (CLuc-NLRP3^{PYD}) to the N-terminus, and *Xho*I enzyme site to the C-terminus of NLRP3^{PYD}. All used primers are detailed in Table 1.

Thereafter, the ligation products (NLuc-NLRP3^{PYD} and CLuc-NLRP3^{PYD}) were transformed into DH5-alpha Competent *E. coli* (BioLabs-C2987I) and screened by antibiotic (100 mg/ml Kanamycin) selection. Positive clones were selected by colony PCR and double digestion and then sequenced (Macrogen, Korea) to ensure inserted DNAs. NLuc-NLRP3^{PYD} S5D and CLuc-NLRP3^{PYD} S5D mutants were constructed using the appropriate primers and splicing by overlap extension PCR (SOE-PCR). All genes were amplified by Pfu DNA polymerase and then cloned into the pET28a (+) expression vector by T4 DNA ligase. Enzymes were purchased from BioLabs (UK).

2.2. Structural superimposition

Molecular docking of NLRP3^{PYD}-NLRP3^{PYD} homodimer interaction was performed with HADDOCK (High Ambiguity Driven protein-protein DOCKing) web server [33] using crystal structure of NLRP3^{PYD} (Protein Data Bank ID code 3QF2 (chain A)) as template. Active residues were determined by referring to previous study [34] and surface exposure of these residues were calculated by GETAREA [35] with 30% solvent accessibility threshold. The interfaces that specified for interaction were formed by α-helices H1 and H4 (residues Ser 5, Arg 7, Cys 8, Glu 15, Asp 50, Val 52, Asp 53 and Thr 56) of one NLRP3^{PYD} molecule and residues from H2 (Lys 23, Lys 24, Met 27 and Asp 31) of the other NLRP3^{PYD}. All other HADDOCK parameters were left unchanged to their respective default values in docking procedure. In each docking, the conformation with the lowest energy cluster was chosen as the docked model for the next analysis.

Modelling of mutation (Ser to Asp) and phosphorylation of Ser 5 was carried out manually by Maestro release 2020-4 (version 12.6, Schrodinger, LLC, New York, NY, 2020) software. Structural superimposition of native and mutant docked models was analyzed by PYMOL v.2.3.3. Poisson-Boltzmann electrostatic potential surfaces were calculated by Maestro. All structures and docking results visualized and modelled using PYMOL v 2.3.3 and Maestro.

2.3. Protein expression and purification

BL21 (DE3) competent *E. coli* (BioLabs-C2527H) was used to express the proteins. Bacterial cells were grown in 2xYT (Yeast Extract Tryptone) medium. In $OD600 = 0.7$, the protein expression was induced by adding 0.5 mM IPTG (Sigma-Aldrich-367-93-1) and cultivation continued with reciprocal shaking (180 RPM) at 20 °C for 16 h. NLuc-NLRP3^{PYD}, CLuc-NLRP3^{PYD} and their mutants, as well as ASC protein were purified from *E. coli* cell pellets after centrifugation (5000 RPM, 20 min). Cell lysis was continued by sonication in a lysis buffer including 20 mM Tris (pH 7.8), 500 mM NaCl and 5 mM imidazole. Since ASC protein was in the inclusion bodies, the pellets were lysed in the lysis buffer containing 8 M urea, pH 8.0. After sonication, the centrifuge was performed, and the supernatant was used for purification. Because of a polyhistidine tag at the N-terminus of NLuc-NLRP3^{PYD}, CLuc-NLRP3^{PYD}, their mutants, and ASC, Ni-NTA-Sepharose chromatography was used for the purification step. Bacterial supernatant was added to the equilibrated Ni-NTA- Sepharose column and the column was washed by washing buffer (20 mM Tris, 500 mM NaCl, 40 mM imidazole, pH 7.8) after 20 min. For ASC protein, re-folding was performed on the Ni-NTA-Sepharose column at a gradient of decreasing urea concentration. In the next step, elution of adsorbed proteins was performed by elution buffer

Table 1
Primers used to generate the constructs.

	Primer sequence 5′–3′
F-NLuc- containing the *Nde*I site	CCCATATGATGGAAGACGCCAAAAAC
R-NLuc- containing the *Sal*I site	TTGTCGACGGCTACCGCCGCCACCGCTGCCACCGCCACCTCCATCCTTGT
F-CLuc- containing the *Nde*I site	CCATGGTTCATATGTCCGGTTATGTAAACAATC
R-CLuc- containing the *Nde*I site	AGCCATATGGCTGCCACCACCGCCGCTACCACCGCCACCGCTACCGCCACCACCGAGCTCCAATTTG
F-NLRP3^{PYD}- containing the *Eco*RI site	TTGAATTCATGAAGATGGCAAGCACCC
F-NLRP3^{PYD}- containing the *Sal*I site	TTGTCGACAAATGAAGATGGCAAGCACCC
R-NLRP3^{PYD}- containing the *Xho*I site	TTCTCGAGTTACTTCGGCTCATCTCTTTTTG
F1- NLuc-NLRP3^{PYD} S5D- containing the *Hin*dIII site	ATAGAAAAGCTTTTATGGAAGACGCCAAAAAC
F1- CLuc-NLRP3^{PYD} S5D- containing the *Hin*dIII site	ATAGAAAAGCTTTTATGTCCGGTTATGTAAAC
R1- NLuc/CLuc-NLRP3^{PYD} S5D	GGGTGTCTGCCATCTTCAT
F2- NLuc/CLuc-NLRP3^{PYD} S5D	GAAGATGGCAGACACCCGCTG
R2- NLuc/CLuc-NLRP3^{PYD} S5D- containing the *Xho*I site	ATAGAACTCGAGTTACTTCGGCTCATC

(20 mM Tris, 300 mM NaCl, 275 mM imidazole, pH 7.8). Expression and purification of proteins were investigated by 12% SDS-PAGE analysis and measurement of total protein concentration was carried out by the Bradford technique.

2.4. Immunoblotting

Bacterial lysis of each constructs was resolved by SDS-PAGE gel. After protein separation by gel electrophoresis, proteins transferred to a nitrocellulose membrane (250 mA for 150 min). The membrane blocking was carried out by 4% skimmed milk in TBST for 1 h at room temperature followed with an overnight incubation with primary antibody at 4 °C. The membrane was washed 3–5 times for 10 min with TBS containing 0.1% Tween 20 (TBST) before incubation with secondary antibody. Mouse anti-6X His Tag antibody was used as primary antibody and goat anti-mouse (Li-cor, 926–68020) was used as secondary antibody. After that, the membrane was scanned using a LICOR system.

2.5. Luciferase activity assay

The proteins containing CLuc (CLuc-NLRP3^{PYD} or CLuc-NLRP3^{PYD} S5D) (0.3 mg/mL) were added in the separate wells of a 96-well plate at first and then, the proteins containing NLuc (NLuc-NLRP3^{PYD} or NLuc-NLRP3^{PYD} S5D) (0.3 mg/mL) were added. The luciferase activity was monitored by using Sirius tube luminometer (Berthold detection systems), as a detectable luminescence signal produced upon addition of 10 μL of luciferase assay complex (25 mM Tris, 10 mM $MgSO_4$, 1 mM luciferin, and 2 mM ATP) to protein mixtures.

2.5.1. Evaluation of the effect of ASC protein in vitro and in cell-based system

In order to evaluate the efficiency of the recombinant proteins for recruiting ASC, full length human ASC was added to the assay mixture. In this experiment, NLuc-NLRP3^{PYD} and CLuc-NLRP3^{PYD} were mixed with different concentration of ASC protein and the luminescence signal was immediately monitored as detailed above.

To confirm the effects of ASC on NLRP3 oligomerization in cell-based system, human embryonic kidney cells (HEK293T; Iranian Biological Resource Center) were cultured in high glucose Dulbecco's Modified Eagle's Medium (Gibco) supplemented with 10% (v/v) fetal bovine serum (FBS; Gibco) and 1% (v/v) penicillin/streptomycin (Gibco). The cells were transiently transfected with pEGFP-C2-NLRP3 (Addgene plasmid # 73955) and pcDNA3.1^{+}-ASC plasmids (250 ng/well of a 24-well plate for each plasmid) with branched 25 kDa polyethylenimine (Sigma-Aldrich). The cell cultures were incubated at 37 °C in an atmosphere with 5% (v/v) CO_2. After 24 h, fluorescence imaging of cells was taken with Cytation™ 3 cell imaging Multi-Mode Reader (BioTek Instruments, USA).

2.5.2. Evaluation of the effect of MCC950 on the luciferase activity of designed reporters

In order to evaluate the effects of MCC950, as an NLRP3 inflammasome inhibitor, on luciferase activity of NLuc-NLRP3^{PYD} and CLuc-NLRP3^{PYD} reporters, CLuc-NLRP3^{PYD} protein was incubated with different concentrations of MCC950 at room temperature. After 15 min, NLuc-NLRP3^{PYD} protein was added to the mixture and luciferase activity was immediately monitored as detailed above.

3. Results and discussion

Bioluminescence assays hold an invaluable role in high-throughput screening methods due to the high sensitivity and wide dynamic ranges of bioluminescence. In the current study, we established an assay based on split luciferase reporters to investigate the homotypic PYD domain of NLRP3 (NLRP3^{PYD}) interactions *in vitro* in order to use this new method to study inflammasome complex formation and identify NLRP3 activators and inhibitors.

3.1. Design and construction of a split luciferase sensor for detecting NLRP3^{PYD}-NLRP3^{PYD} interaction

Based on crystal structure of human NLRP3^{PYD} (PDB ID code: 3QF2), a split luciferase biosensor was designed. Combination of theoretical data and empirically driven structure are needed to create an effective interaction-induced split luciferase reassembly. For this purpose, several factors should be evaluated including the distance between the reporter protein fragments before and after the interaction, the position and orientation of complementary fragments through the complementation of protein dimer after the interaction, and the dissection sites of split luciferase fragments [36,37].

Based on previous studies, the best luciferase complementary fragments are from 1 to 416 and 395 to 550 amino acids as N-terminal and C-terminal fragments respectively [38,39]. In this study, considering these crucial factors and crystal structure of NLRP3 protein containing high affinity PYD domain, an intermolecular assay for monitoring of NLRP3^{PYD}-NLRP3^{PYD} interactions were produced. To enhance the folding and flexibility of luciferase fragments, a flexible linker composed of $(GGGGS)_n$ was inserted at the junction between the luciferase fragments and NLRP3^{PYD} ($(GGGGS)_3$ linker for NLuc and $(GGGGS)_4$ linker for CLuc fragment) (Fig. 1A).

3.2. S5D mutation: a loss of function phosphomimetic mutant

As noted previously, luciferase complementation occurs when two complementary fragments of luciferase bring together in subsequence of protein-protein interaction of two targeted proteins. Alternatively, two luciferase fragments can come together by random collision even the pair of interacting proteins may not interact. Luminescence signals that generated through random collisions are considered as non-specific signal. So, to reveal specific protein interactions, contribution of non-specific luminescence must be determined [40,41]. Because of these concerns, we introduced a disrupting mutation at Ser 5, the first residue in helix 1 involved in inflammasome formation through NLRP3^{PYD} interactions which is mainly based on electrostatic interactions, as reported earlier [34]. So, the interaction between PYDs would be interrupted by introduction of negative charges by phosphorylation or a negatively charged residue such as aspartate at position S5. As shown in Fig. 1B, the electrostatic surface potential of wild type and mutant (S5D) NLRP3^{PYD} and NLRP3^{PYD} with phosphorylated S5 (SEP 5) was checked in order to determine the effect of mutation on the charge distribution of the surface and consequently on PYD-PYD interaction. To better understand, Fig. 1C illustrated the changes in electrostatic surface potential of homotypic NLRP3^{PYD}-NLRP3^{PYD} interaction interface of PYDs. Obviously, the positively charged surface area decreased in mutant (S5D) and phosphorylated S5 NLRP3^{PYD}, while more negatively charged regions displayed around the interface residues. Together, these data show the charge distribution of structures is entirely different, suggesting that the mutation may influence interaction by electrostatic repulsion of two PYDs.

Therefore, to corroborate the reporting abilities of split luciferase complementary system in response to NLRP3^{PYD}-NLRP3^{PYD} interaction, the biosensor harboured NLRP3^{PYD} mutation [NLuc-NLRP3^{PYD} S5D and CLuc-NLRP3^{PYD} S5D] was prepared as a disrupting control mutant. As indicated in Fig. 1D, superimposition of NLRP3^{PYD} and NLRP3^{PYD} S5D structures with RMSD value of 1.071 indicated no significant conformational changes and suggested a stable structural orientation before and after mutation. It should be noted other NLRP3 mutant could also be used for further NLRP3 homotypic interaction and heterotypic interaction with ASC. For example, NLRP3 Y32 mutants were able to bind to WT NLRP3 in HEK 293T cells, suggesting that NLRP3 dephosphorylation at Tyr 32 is not necessary for NLRP3 oligomerization, while it was found that NLRP3 Y32D or NLRP3 Y32E could not recruit ASC, suggesting that

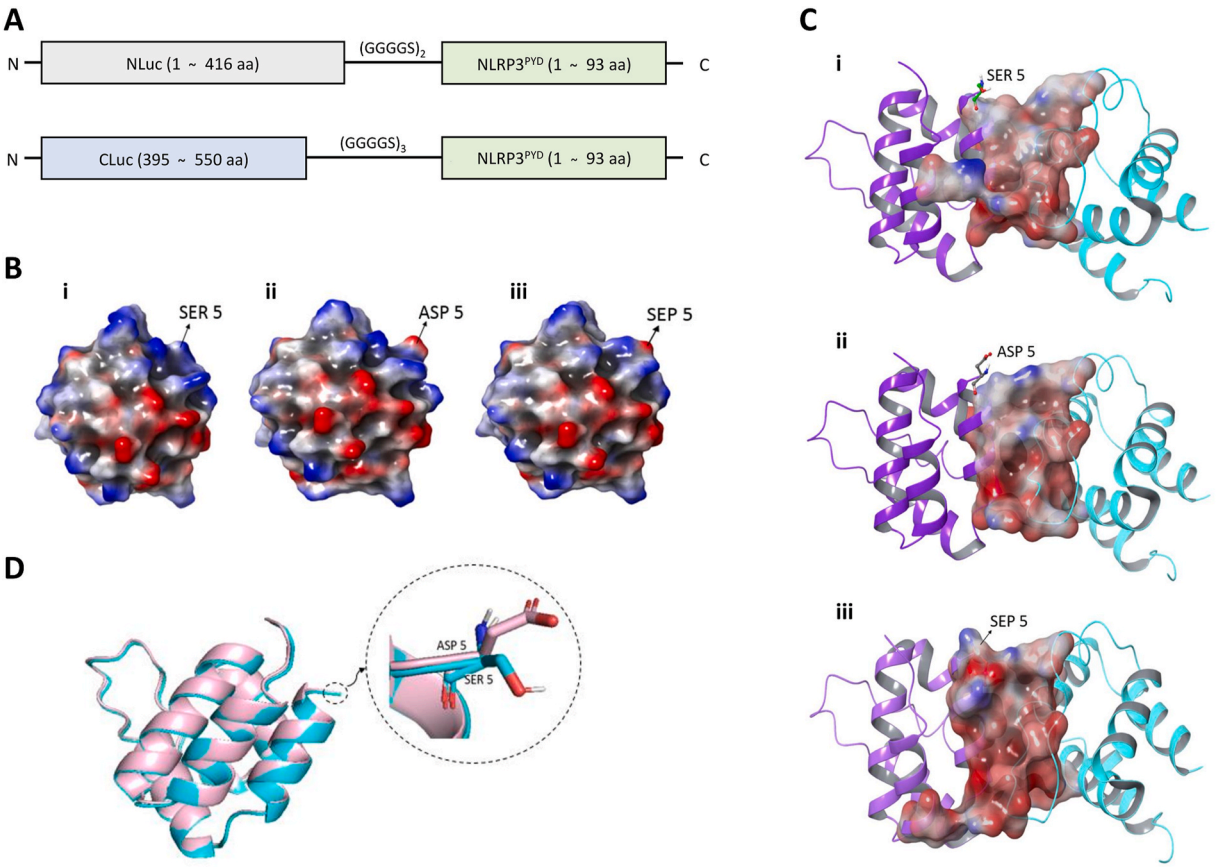

Fig. 1. A) General scheme of constructs with the split luciferase fragments (NLuc and CLuc). The N-terminal fragment of firefly luciferase (1–416 amino acids) connected to N-terminus of NLRP3^{PYD} through $(GGGGS)_2$ flexible linker and the C-terminal fragment of firefly luciferase (395–550 amino acids) connected to N-terminus of NLRP3^{PYD} through $(GGGGS)_3$ linker. B) The electrostatic surface potential of wild type (i), S5D mutant (ii) and phosphorylated S5 (iii) NLRP3^{PYD}s (PDB ID code:3QF2), with the same orientation. Positive and negative charged residues have been represented by blue and red areas; respectively. C) The changes in electrostatic surface potential of homotypic NLRP3^{PYD}-NLRP3^{PYD} interaction interface of wild type (i), S5D mutant (ii) and phosphorylated S5 (iii) NLRP3^{PYD}s with the same orientation. The surface is characterized ranging from positive electrostatic potential (blue surface) to a negative potential (red surface) with 30% transparency. In i and ii, Ser and Asp residues are shown in ball and stick representation. D) Structural comparison of wild type NLRP3^{PYD} (cyan) and its S5D mutant (light pink) on helix H1 has performed by superimposition of structures using PYMOL. Inset shows the zoomed version of wild type and mutant residue in stick representation. (For interpretation of the references to colour in this figure legend, the reader is referred to the Web version of this article.)

NLRP3 dephosphorylation at Tyr 32 is a prerequisite for NLRP3–ASC interaction [42].

Expression and purification of NLuc-NLRP3^{PYD}, CLuc-NLRP3^{PYD} and their S5D mutants were done as described at general scheme of Fig. 2A. As shown in Fig. 2B and C, CLuc-NLRP3^{PYD}, NLuc-NLRP3^{PYD} and mutated forms were purified by Ni-NTA-Sepharose. Based on SDS-PAGE gel results, NLuc-NLRP3^{PYD} and its mutant form showed an estimated MW about 60 kDa. CLuc-NLRP3^{PYD} and its mutated form showed a molecular weight of about 35 kDa. Also, expression of NLuc-NLRP3^{PYD} and CLuc-NLRP3^{PYD} was confirmed through western blotting using an antibody against 6X His Tag (Fig. 2D).

3.3. Reconstitution of luciferase activity through PYD-PYD interaction

It is clearly shown that the NLRP3^{PYD} domain has a dual binding role in which both recruits ASC via PYD–PYD interaction and binds to another NLRP3^{PYD} domain and it is therefore required for the formation of the active inflammasome complex [10]. Moreover, Crystal structure of NLRP3 protein Pyrin domain (PYD) shows, it has a six-helical bundle structural fold containing several conserved residues as compared to other PYD domains interacting with ASC and with a possible homodimeric interface [6]. NLRP3 inflammasome has been considered as an attractive target for the development of NLRP3 inhibitors [43].

Therefore, we hypothesized that due to the interaction of NLRP3^{PYD}s, the N-terminal and C-terminal fragments of luciferase would interact, and the functional structure of the firefly luciferase would be reconstituted leading to luminescence activity. In order to test our designed reporter, the luciferase activity of NLuc-NLRP3^{PYD}/CLuc-NLRP3^{PYD} and NLuc-NLRP3^{PYD} S5D/CLuc-NLRP3^{PYD} S5D were measured after simple mixing of purified proteins. Moreover, luciferase activity of each fragment separately was detected as specificity controls. As demonstrated in Fig. 2E, separate constructs did not result in detectable luminescence recovery, indicating that the luciferase fragments alone have no significant activity. While, both luciferase fragments of NLuc-NLRP3^{PYD}/CLuc-NLRP3^{PYD} brought about a high level of luminescence signal, reflect NLRP3^{PYD} oligomerization in the assay mixture. Luciferase activity was totally abolished when S5 was mutated to the phosphomimetic aspartate in NLuc-NLRP3^{PYD} S5D/CLuc-NLRP3^{PYD} S5D mixture. Indeed, mutant NLRP3^{PYD} S5D cannot make homotypic interactions. That is to say, reconstitution of luciferase activity was due to right juxtaposition of PYD domains and their productive interactions. It is noteworthy that a recent report for monitoring of α-synuclein interactions using split luciferase complementation assay confirmed that right orientation of interacting targeting molecules is crucial in induction of split-luciferase activity [44]. Using ASC as second player in NLRP3 inflammasome shows saturating concentration of ASC in the assay medium brought about with a moderate increase in luciferase complementary activity which is more supported with Speck-like

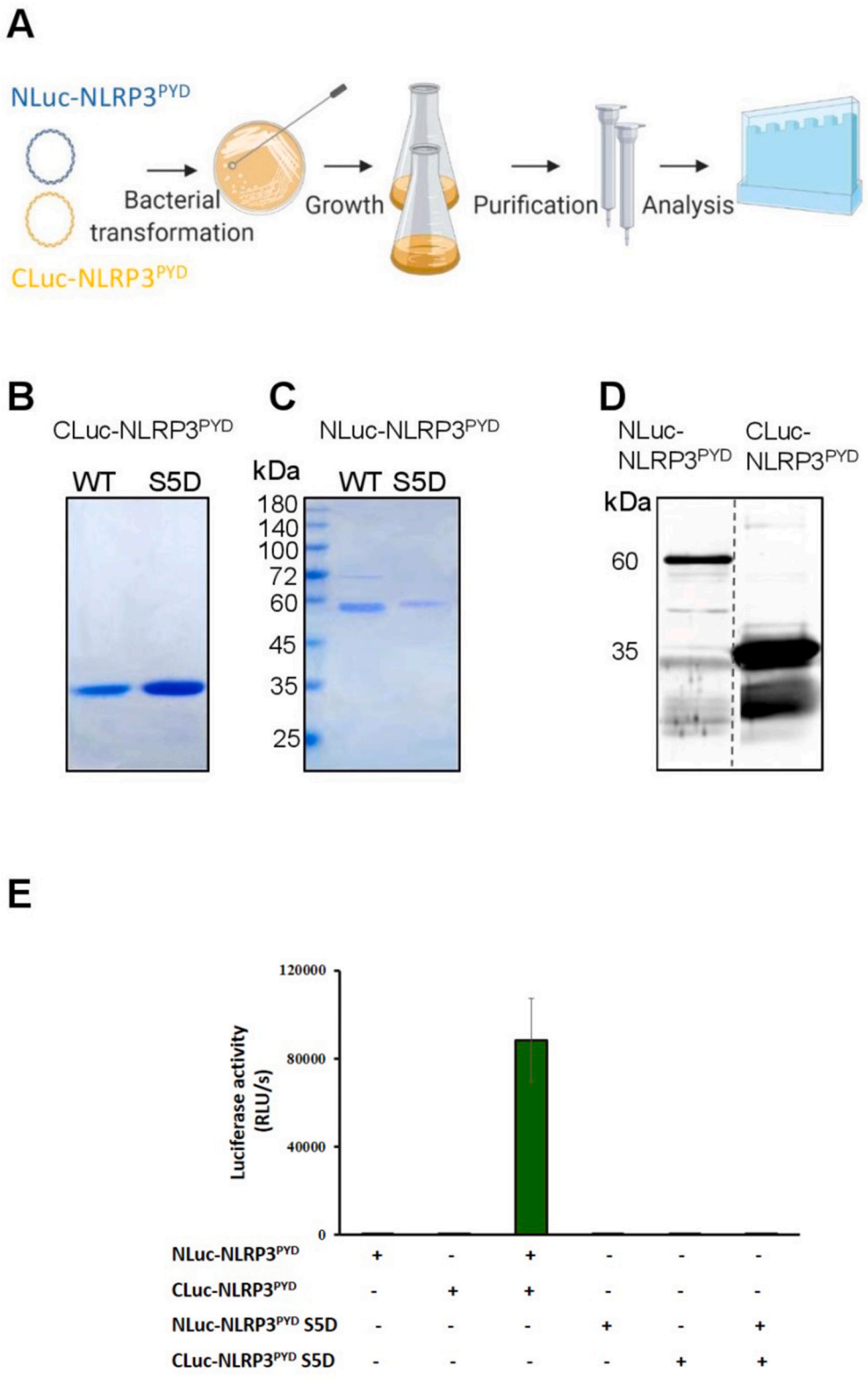

Fig. 2. A) General scheme of expression and purification of constructs. B) SDS-PAGE of purified CLuc-NLRP3^{PYD} and CLuc-NLRP3^{PYD} S5D; and C) NLuc-NLRP3^{PYD} and NLuc-NLRP3^{PYD} S5D via affinity Ni-NTA-Sepharose column chromatography. D) Immunoblot analysis of NLRP3^{PYD} constructs confirmed expression of NLuc-NLRP3^{PYD} and CLuc-NLRP3^{PYD} through western blotting using an antibody against 6X His Tag E) Relative split-luciferase complementary assay. The luciferase activity was performed for 30 min and maximum luciferase activity was reported. RLU refers to relative luminescence units. Data are the mean ± SD of three independent experiments.

formation with co-transfection of GFP-NRP3 and ASC (Fig. 3). In fact, it may be suggested expression of ASC in presence of NLRP3 lead to stronger assembly of NLRP3 and inflammasome formation, as further supported by higher Pyd-Pyd interaction *in vitro* condition (Fig. 3). It should be pointed out that observed ASC effect on luciferase complementation were obtained at high salt conecntration of elution buffer (275 mM imidazol and 300 mM NaCl) which may be different in other buffer concentrations. However, the effect of different concentration of ASC on free firefly luciferase showed luciferase activity was not decreased in presence of exogenous ASC protein.

It should be pointed out, the effect of a known inflammasome inhibitor (MCC950) on split luciferase complementation assay as an indicator of Pyd-Pyd assembly up to 10 μM was also monitored which showed no significant effect. It has been shown that MCC950 as a potent

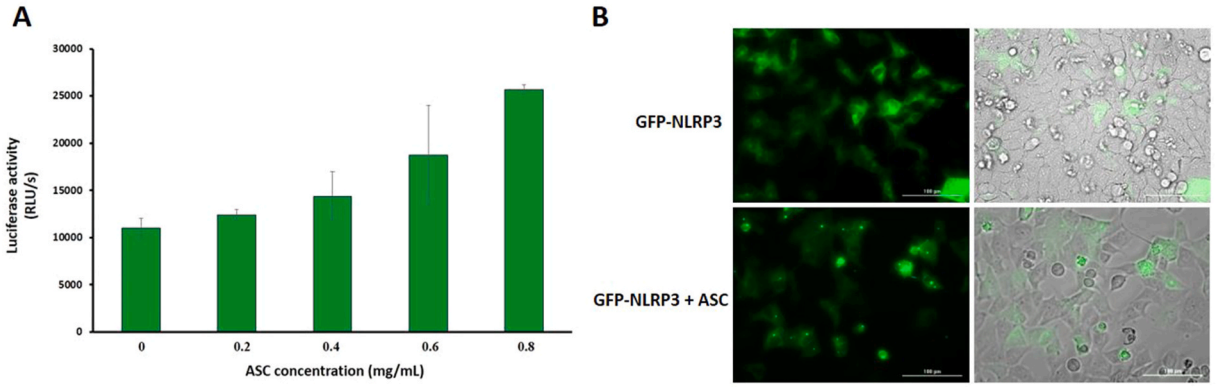

Fig. 3. A) Effects of different concentrations of ASC protein (0–0.8 mg/mL) on the luciferase activity of NLuc-NLRP3^{PYD} and CLuc-NLRP3^{PYD} reporters. B) Effects of ASC proteins on the oligomerization of GFP-NLRP3 in transfected HEK293T cells. Cells transfected with GFP-NLRP3 and ASC formed puncta.

and specific small-molecule inhibitor of the NLRP3 pathway directly interacts with the Walker B motif within the NLRP3 NACHT domain, thereby blocking ATP hydrolysis and inhibiting NLRP3 activation and inflammasome formation [45]. Therefore, lack of inhibition of Pyd-Pyd interaction through even higher concentration of MCC950 could be expected.

4. Conclusion

According to the results presented in this manuscript, split luciferase complementation assay is an efficient method to monitor the NLRP3^{PYD} homo-interactions. Previous reported sensor for homo-oligomerization of NLRP3 based on BRET assay has been reported [46]. However, need of cell-based expression of reporters, high cost and heterogeneous intracellular microenvironment makes high throughput screening of chemical libraries difficult to be achieved. However, recombinant bacterial-based expression and affinity chromatography brought about an easy procedure to obtain a remarkable quantity of purified NLRP3^{PYD} domains for future screening analyses. While the native PYD domain of NLRP3 has the ability to homo-oligomerize and reconstitute luciferase activity, the phosphomimetic mutant form, NLRP3^{PYD} S5D, disrupts the oligomer and does not show luciferase activity, reinforcing the reliability of the NLRP3^{PYD} split luciferase complementation assay as a reliable method to study NLRP3^{PYD} self-assembly. This assay could be easily adapted to high throughput screening format providing a new method to identify drugs targeting the NLRP3^{PYD} domain and further investigation of NLRP3 structure as performed for Apaf-1 [47].

CRediT authorship contribution statement

Mohsen Isazadeh: He performed experiments. **Mojdeh Amandadi:** She designed and made mutant and ASC assay concept. **Farnaz Haghdoust:** experimental support. **Shima Lotfollazadeh:** structural modelling, reading. **Mar Orzáez:** She provided original plasmids, Formal analysis, interpretation. **Saman Hosseinkhani:** experimental design, writing and funding, model concept.

Acknowledgment

Financial support of this work is provided by research council of Tarbiat Modares University through a grant (#IG/39803) to cell death and differentiation research program.

References

[1] T.-D.K. Patrick, J. Shaw, Michael F. McDermott, inflammasomes and autoimmunity, Trends Mol. Med. 17 (2011) 57–64, https://doi.org/10.1016/j.molmed.2010.11.001.

[2] Haitao Guo, Justin B. Callaway, Jenny P.-Y Ting, Inflammasomes: mechanism of action, role in disease, and therapeutics, Nat. Med. 21 (2016) 677–687, https://doi.org/10.1038/nm.3893.

[3] S.L. Fink, B.T. Cookson, Caspase-1-dependent pore formation during pyroptosis leads to osmotic lysis of infected host macrophages, Cell Microbiol. 8 (2006) 1812–1825, https://doi.org/10.1111/j.1462-5822.2006.00751.x.

[4] A. Lu, H. Wu, Structural mechanisms of inflammasome assembly, FEBS J. 282 (2015) 435–444, https://doi.org/10.1111/febs.13133.

[5] T. Bergsbaken, S.L. Fink, B.T. Cookson, Pyroptosis: host cell death, Nat. Rev. Microbiol. 7 (2009) 99–109, https://doi.org/10.1038/nrmicro2070.

[6] J.Y. Bae, H.H. Park, Crystal structure of NALP3 Protein Pyrin Domain (PYD) and its implications in inflammasome assembly, J. Biol. Chem. 286 (2011) 39528–39536, https://doi.org/10.1074/jbc.M111.278812.

[7] J.M. Elliott, L. Rouge, C. Wiesmann, J.M. Scheer, Crystal structure of procaspase-1 zymogen domain reveals insight into inflammatory caspase autoactivation, J. Biol. Chem. 284 (2009) 6546–6553, https://doi.org/10.1074/jbc.M806121200.

[8] E. de Alba, Structure and interdomain dynamics of apoptosis-associated speck-like protein containing a CARD (ASC), J. Biol. Chem. 284 (2009) 32932–32941, https://doi.org/10.1074/jbc.M109.024273.

[9] L. Sborgi, F. Ravotti, V.P. Dandey, M.S. Dick, A. Mazur, S. Reckel, M. Chami, S. Scherer, M. Huber, A. Böckmann, E.H. Egelman, H. Stahlberg, P. Broz, B. H. Meier, S. Hiller, Structure and assembly of the mouse ASC inflammasome by combined NMR spectroscopy and cryo-electron microscopy, Proc. Natl. Acad. Sci. U. S. A 112 (2015) 13237–13242, https://doi.org/10.1073/pnas.1507579112.

[10] J. Oroz, S. Barrera-Vilarmau, C. Alfonso, G. Rivas, E. De Alba, ASC pyrin domain self-associates and binds NLRP3 protein using equivalent binding interfaces, J. Biol. Chem. 291 (2016), https://doi.org/10.1074/jbc.M116.741082, 19487–19501.

[11] P.R. Vajjhala, R.E. Mirams, J.M. Hill, Multiple binding sites on the pyrin domain of ASC protein allow self-association and interaction with NLRP3 protein, J. Biol. Chem. 287 (2012) 41732–41743, https://doi.org/10.1074/jbc.M112.381228.

[12] P.R. Vajjhala, S. Kaiser, S.J. Smith, Q.R. Ong, S.L. Soh, K.J. Stacey, J.M. Hill, Identification of multifaceted binding modes for pyrin and ASC pyrin domains gives insights into pyrin inflammasome assembly, J. Biol. Chem. 289 (2014) 23504–23519, https://doi.org/10.1074/jbc.M114.553305.

[13] P. Broz, V.M. Dixit, Inflammasomes: mechanism of assembly, regulation and signalling, Nat. Rev. Immunol. 16 (2016) 407–420, https://doi.org/10.1038/nri.2016.58.

[14] A.S. Pinheiro, C. Eibl, Z. Ekman-Vural, R. Schwarzenbacher, W. Peti, The NLRP12 pyrin domain: structure, dynamics, and functional insights, J. Mol. Biol. 413 (2011) 790–803, https://doi.org/10.1016/j.jmb.2011.09.024.

[15] L.H. Chu, A. Gangopadhyay, A. Dorfleutner, C. Stehlik, An updated view on the structure and function of PYRIN domains, Apoptosis 20 (2015) 157–173, https://doi.org/10.1007/s10495-014-1065-1.

[16] T. Jin, A. Perry, P. Smith, J. Jiang, T.S. Xiao, Structure of the absent in melanoma 2 (AIM2) pyrin domain provides insights into the mechanisms of AIM2 autoinhibition and inflammasome assembly, J. Biol. Chem. 288 (2013) 13225–13235, https://doi.org/10.1074/jbc.M113.468033.

[17] S. Hiller, A. Kohl, F. Fiorito, T. Herrmann, G. Wider, J. Tschopp, M.G. Grütter, K. Wüthrich, NMR structure of the apoptosis- and inflammation-related NALP1 pyrin domain, Structure 11 (2003) 1199–1205, https://doi.org/10.1016/j.str.2003.08.009.

[18] E. Liepinsh, R. Barbals, E. Dahl, A. Sharipo, E. Staub, G. Otting, The death-domain fold of the ASC PYRIN domain, presenting a basis for PYRIN/PYRIN recognition, J. Mol. Biol. 332 (2003) 1155–1163, https://doi.org/10.1016/j.jmb.2003.07.007.

[19] A. Natarajan, R. Ghose, J.M. Hill, Structure and dynamics of ASC2, a pyrin domain-only protein that regulates inflammatory signaling, J. Biol. Chem. 281 (2006) 31863–31875, https://doi.org/10.1016/s0021-9258(19)84101-7.

[20] A.S. Pinheiro, M. Proell, C. Eibl, R. Page, R. Schwarzenbacher, W. Peti, Three-dimensional structure of the NLRP7 pyrin domain insight into pyrin-pyrin-mediated effector domain signaling in innate immunity, J. Biol. Chem. 285 (2010) 27402–27410, https://doi.org/10.1074/jbc.M110.113191.

[21] C. Eibl, S. Grigoriu, M. Hessenberger, J. Wenger, S. Puehringer, A.S. Pinheiro, R. N. Wagner, M. Proell, J.C. Reed, R. Page, K. Diederichs, W. Peti, Structural and functional analysis of the NLRP4 pyrin domain, Biochemistry 51 (2012) 7330–7341, https://doi.org/10.1021/bi3007059.
[22] M.Y. Su, C.I. Kuo, C.F. Chang, C.I. Chang, Three-dimensional structure of human NLRP10/PYNOD pyrin domain reveals a homotypic interaction site distinct from its mouse homologue, PLoS One 8 (2013) 1–9, https://doi.org/10.1371/journal.pone.0067843.
[23] C. Eibl, M. Hessenberger, J. Wenger, H. Brandstetter, Structures of the NLRP14 pyrin domain reveal a conformational switch mechanism regulating its molecular interactions, Acta Crystallogr. Sect. D Biol. Crystallogr. 70 (2014), https://doi.org/10.1107/S1399004714010311, 2007–2018.
[24] M. Hattori, T. Ozawa, Split luciferase complementation for analysis of intracellular signaling, Anal. Sci. 30 (2014) 539–544, https://doi.org/10.2116/analsci.30.539.
[25] T. Azad, A. Tashakor, S. Hosseinkhani, Split-luciferase complementary assay: applications, recent developments, and future perspectives, Anal. Bioanal. Chem. 406 (2014) 5541–5560, https://doi.org/10.1007/s00216-014-7980-8.
[26] M. Torkzadeh-mahani, F. Ataei, M. Nikkhah, S. Hosseinkhani, Design and development of a whole-cell luminescent biosensor for detection of early-stage of apoptosis, Biosens. Bioelectron. 38 (2012) 362–368, https://doi.org/10.1016/j.bios.2012.06.034.
[27] A.R. Noori, E.S. Hosseini, M. Nikkhah, S. Hosseinkhani, Apoptosome formation upon overexpression of native and truncated Apaf-1 in cell-free and cell-based systems, Arch. Biochem. Biophys. 642 (2018) 46–51, https://doi.org/10.1016/j.abb.2018.01.017.
[28] E.S. Hosseini, M. Nikkhah, A.A. Hamidieh, H.O. Fearnhead, J.P. Concordet, S. Hosseinkhani, The Lumiptosome, an engineered luminescent form of the apoptosome can report cell death by using the same Apaf-1 dependent pathway, J. Cell Sci. 133 (2020), https://doi.org/10.1242/jcs.242636.
[29] A.R. Noori, A. Tashakor, M. Nikkhah, L.A. Eriksson, S. Hosseinkhani, H. O. Fearnhead, Loss of WD2 subdomain of Apaf-1 forms an apoptosome structure which blocks activation of caspase-3 and caspase-9, Biochimie 180 (2021) 23–29, https://doi.org/10.1016/j.biochi.2020.10.013.
[30] A. Tashakor, M. H-Dehkordi, E. O'Connell, S. Gomez Ganau, R. Gozalbes, L. A. Eriksson, S. Hosseinkhani, H.O. Fearnhead, A new split-luciferase complementation assay identifies pentachlorophenol as an inhibitor of apoptosome formation, FEBS Open Bio 9 (2019) 1194–1203, https://doi.org/10.1002/2211-5463.12646.
[31] M. Takeuchi, Y. Nagaoka, T. Yamada, H. Takakura, T. Ozawa, Ratiometric bioluminescence indicators for monitoring cyclic adenosine 3′,5′-monophosphate in live cells based on luciferase-fragment complementation, Anal. Chem. 82 (2010) 9306–9313, https://doi.org/10.1021/ac102692u.
[32] N. Misawa, A.K.M. Kafi, M. Hattori, K. Miura, K. Masuda, T. Ozawa, Rapid and high-sensitivity cell-based assays of protein-protein interactions using split click beetle luciferase complementation: an approach to the study of G-protein-coupled receptors, Anal. Chem. 82 (2010) 2552–2560, https://doi.org/10.1021/ac100104q.
[33] S.J. De Vries, M. Van Dijk, A.M.J.J. Bonvin, The HADDOCK web server for data-driven biomolecular docking, Nat. Protoc. 5 (2010) 883–897, https://doi.org/10.1038/nprot.2010.32.
[34] A. Stutz, C.C. Kolbe, R. Stahl, G.L. Horvath, B.S. Franklin, O. van Ray, R. Brinkschulte, M. Geyer, F. Meissner, E. Latz, NLRP3 inflammasome assembly is regulated by phosphorylation of the pyrin domain, J. Exp. Med. 214 (2017) 1725–1736, https://doi.org/10.1084/jem.20160933.
[35] R. Fraczkiewicz, W. Braun, Exact and efficient analytical calculation of the accessible surface areas and their gradients for macromolecules, J. Comput. Chem. 19 (1998) 319–333. https://doi.org/10.1002/(SICI)1096-987X(199802).
[36] B.K. Sung, Y. Otani, Y. Umezawa, H. Tao, Bioluminescent indicator for determining protein-protein interactions using intramolecular complementation of split click beetle luciferase, Anal. Chem. 79 (2007) 4820–4826, https://doi.org/10.1021/ac0621571.
[37] S.S.G. Ramasamy Paulmurugan, Firefly luciferase enzyme fragment complementation for imaging in cells and living animals, Anal. Chem. 77 (2005) 1295–1302, https://doi.org/10.1021/ac0484777.
[38] R. Paulmurugant, S.S. Gambhir, Monitoring protein-protein interactions using split synthetic renilla luciferase protein-fragment-assisted complementation, Anal. Chem. 75 (2003) 1584–1589, https://doi.org/10.1021/ac020731c.
[39] K.E. Luker, M.C.P. Smith, G.D. Luker, S.T. Gammon, H. Piwnica-worms, D. Piwnica-worms, Kinetics of regulated protein – protein interactions revealed with firefly luciferase complementation imaging in cells and living animals, Proc. Natl. Acad. Sci. U. S. A. 101 (2004). https://doi.org/10.1073/pnas.0404041101.
[40] Y. Kodama, C.D. Hu, Bimolecular fluorescence complementation (BiFC): a 5-year update and future perspectives, Biotechniques 53 (2012) 285–298, https://doi.org/10.2144/000113943.
[41] M. Walter, C. Chaban, K. Schütze, O. Batistic, K. Weckermann, C. Näke, D. Blazevic, C. Grafen, K. Schumacher, C. Oecking, K. Harter, J. Kudla, Visualization of protein interactions in living plant cells using bimolecular fluorescence complementation, Plant J. 40 (2004) 428–438, https://doi.org/10.1111/j.1365-313X.2004.02219.x.
[42] Y. Huang, H. Wang, Y. Hao, H. Lin, M. Dong, J. Ye, L. Song, Y. Wang, Q. Li, B. Shan, Y. Jiang, H. Li, Z. Shao, G. Kroemer, H. Zhang, L. Bai, T. Jin, C. Wang, Y. Ma, Y. Cai, C. Ding, S. Liu, Y. Pan, W. Jiang, R. Zhou, Myeloid PTEN promotes chemotherapy-induced NLRP3-inflammasome activation and antitumour immunity, Nat. Cell Biol. 22 (2020) 716–727, https://doi.org/10.1038/s41556-020-0510-3.
[43] G. Yang, H.E. Lee, S.J. Moon, K.M. Ko, J.H. Koh, J.K. Seok, J.K. Min, T.H. Heo, H. C. Kang, Y.Y. Cho, H.S. Lee, K.A. Fitzgerald, J.Y. Lee, Direct binding to NLRP3 pyrin domain as a novel strategy to prevent NLRP3-driven inflammation and Gouty arthritis, Arthritis Rheum. 72 (2020) 1192–1202, https://doi.org/10.1002/art.41245.
[44] S. Mohammadi, M. Nikkhah, S. Hosseinkhani, Investigation of the effects of carbon-based Nanomaterials on A53T alpha-Synuclein aggregation using a whole-cell recombinant biosensor, Int. J. Nanomed. 12 (2017) 8831–8840, https://doi.org/10.2147/IJN.S144764.
[45] R.C. Coll, J.R. Hill, C.J. Day, A. Zamoshnikova, D. Boucher, N.L. Massey, J. L. Chitty, J.A. Fraser, M.P. Jennings, A.A. Robertson, K. Schroder, MCC950 directly targets the NLRP3 ATP-hydrolysis motif for inflammasome inhibition, Nat. Chem. Biol. 15 (2019) 556–559, https://doi.org/10.1038/s41589-019-0277-7.
[46] F. Martín-Sánchez, V. Compan, P. Pelegrín, Measuring NLR oligomerization III: detection of NLRP3 complex by bioluminescence resonance energy transfer, Methods Mol. Biol. 1417 (2016) 159–168, https://doi.org/10.1007/978-1-4939-3566-6-10.
[47] F. Sahebazzamani, S. Hosseinkhani, L.A. Eriksson, H.O. Fearnhead, Apoptosome formation through disruption of the K192-D616 salt bridge in the Apaf-1 closed form, ACS Omega 6 (2021) 22551–22558, https://doi.org/10.1021/acsomega.1c02274.